J Mater Sci (2009) 44:4389–4393
DOI 10.1007/s10853-009-3661-y

Microstructural and mechanical behavior of Zr-based metallic glasses with the addition of Nb

X. M. Luo · Y. Zhou · J. Q. Lu · G. S. Yu · J. G. Lin · W. Li

Received: 21 January 2009 / Accepted: 2 June 2009 / Published online: 23 June 2009

Abstract The effect of Nb content on the microstructure and mechanical properties of Zr-based bulk metallic glass (BMG) were investigated. The addition of Nb led to the formation of the Zr-based metallic glass composites with a ductile dentritic phase by in situ precipitation. The presence of the in situ precipitated phase enhanced significantly the plasticity of the composite under uniaxial compressive test. The interactions between the precipitated phase and the shear band affect the deformation mechanism and fracture mode of the BMG by enhancing the affecting level of the normal stress on the shear surface, and the constant α in the Mohr–Coulomb criterion can reflect the extent of the interactions among particles and the amorphous matrix.

Introduction

Bulk metallic glasses (BMGs) are of scientific and industrial interest because of their unique physical, chemical, and mechanical properties, such as extremely high strength, low elastic modulus, high wear resistance and corrosion resistance, etc. [1–3]. However, the plastic deformation of BMGs is localized in narrow shear bands, followed by the rapid propagation of these shear bands and sudden fracture. As a result, BMGs usually exhibit a poor room temperature ductility, and thus it limits their application of BMGs as structural materials. Therefore, to improve the ductility of these monolithic BMGs is a hot research topic in this field [4–7]. One effective way to improve the ductility of BMGs is to develop BMG based composites, such as composites reinforced with refractory metals or metal fibers, ceramic particles or carbon nanotubes, in situ formed ductile dendritic phase or in situ formed nanocrystals. It has been well documented that these reinforced phases can hinder the propagation of the single shear band within BMGs and seed the initiation of multiple shear bands throughout the specimens, and consequently change the fracture mode of BMGs [8–13]. Thus, investigating the effects of the microstructure of BMG based composites on the mechanical behavior and fracture mode is helpful to optimize the properties of BMG composites by controlling the microstructure. In this study, the BMG based composite, $Zr_{55}Cu_{15.5}Al_{7.5}Ni_{10}Be_{12}$ BMG with different volume fractions of Nb phases, was made through addition of different contents of Nb, and the mechanical behavior and fracture mode were investigated, aiming at elucidating the influence of the volume fraction of the crystalline phase within the BMG on the mechanical behavior and fracture mode.

Experimental

Alloy ingots with the nominal compositions of $(Zr_{55}Cu_{15.5}Al_{7.5}Ni_{10}Be_{12})_{100-x}Nb_x$ ($x = 0$, 5 and 10 in atom percent

X. M. Luo
Physics Department, Tsinghua University, Beijing 100084, People's Republic of China

Y. Zhou · J. Q. Lu
Physics Department, Nanjing University, Nanjing 210093, People's Republic of China

G. S. Yu · J. G. Lin (✉)
Faculty of Material and Photoelectronic Physics, Key Laboratory of Low Dimensional Materials and Application Technology (Ministry of Education), Xiangtan University, Hunan, Xiangtan 411105, People's Republic of China

W. Li (✉)
School of Chemical and Materials Engineering, Huangshi Institute of Technology, Huangshi 435003, People's Republic of China
e-mail: wenl@ualberta.ca

thereafter) were prepared from elemental metals (purity > 99.5%) by arc-melting under the Ti gettered Ar atmosphere. The final alloys were obtained by injecting the liquid metals into a copper mould with a diameter of 3 mm and a length of 50 mm. The structures of the as-cast samples with the different Nb concentrations were characterized by X-ray diffraction (XRD). The compression tests were performed in an Instron-type testing machine at a strain rate of 2×10^{-3} s^{-1} at room temperature. Scanning electron microscopy (SEM) was used to examine the microstructure, the fractography and the shear band morphology near the fracture surface of all the samples.

Results and discussion

Figure 1 shows the XRD patterns of the as-cast samples with the different Nb concentrations. The Nb-free alloy is basically amorphous, as indicated by a broad typical diffusion halo with the absence of any detectable crystalline peaks. However, the XRD patterns for the alloys with 5% Nb are composed of a broad diffusion background and a set of several sharp crystalline peaks, corresponding to a mixture of the amorphous matrix and the precipitated phases. The crystalline phases are indentified to be β-Zr solid solution with a body-centered cubic (bcc) structure. It implies that the crystalline β-Zr phases in situ precipitated during casting. The crystalline diffraction peaks are more pronounced when Nb content increases up to 10%, implying the volume fraction of β-Zr in the alloy increases with the increase of Nb content. It has been proved that Nb is an element to stabilize β phase in Ti- or Zr-base alloys in previous literature [14, 15]. The addition Nb to Zr-based BMGs can promote the β phase precipitation, and β phase is a Zr solid solution, which contains Nb [14]. The present result provided further evidence for this argument, because with the Nb content increasing, the volume fraction of β phases increases dramatically. Figure 2 shows the SEM microstructures of all the samples. The Nb-free amorphous alloy exhibited a featureless structure. While, in the alloy containing 5% alloy, it can be clearly seen the precipitated phase dispersed in the amorphous matrix with some fish-bone-like dendrites (Fig. 2a). With the Nb content of the alloy increasing to 10%, the size and the volume fraction of the dendritic phase both increased significantly. The dendritic β phase was characterized by primary dendrite axes with lengths of 10–20 μm and diameters of about 5 μm (see Fig. 2). The volume fractions of the β-Zr phase are estimated to be about 19 and 42% for the alloys with 5 and 10% Nb, respectively. The SEM observation result is very much in agreement with that of the XRD analysis. This also indicates that the size and morphology of the β phases are strongly dependent on the Nb content.

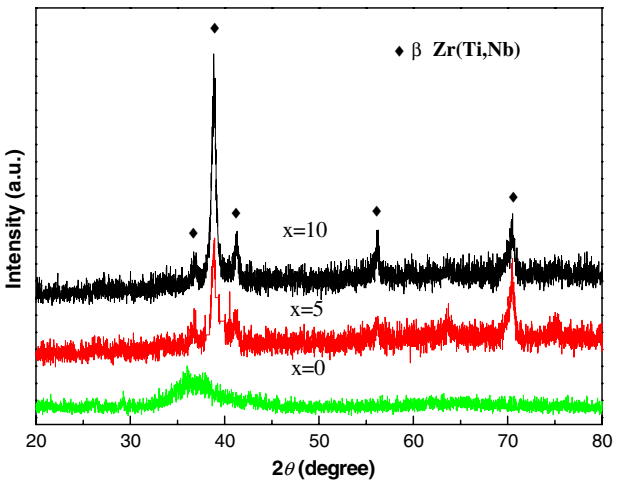

Fig. 1 X-ray diffraction patterns of the monolithic amorphous alloy and bulk metallic glass matrix composites

Figure 3 showed the room temperature compressive stress–strain curves of the samples with different Nb contents at a strain rate of 2×10^{-3} s^{-1} at room temperature. The Nb-free alloy displays only an elastic deformation behavior and catastrophic fracture without distinct plastic deformation. By contrast, the alloys containing 5 and 10% Nb exhibit a quite different deformation feature at same

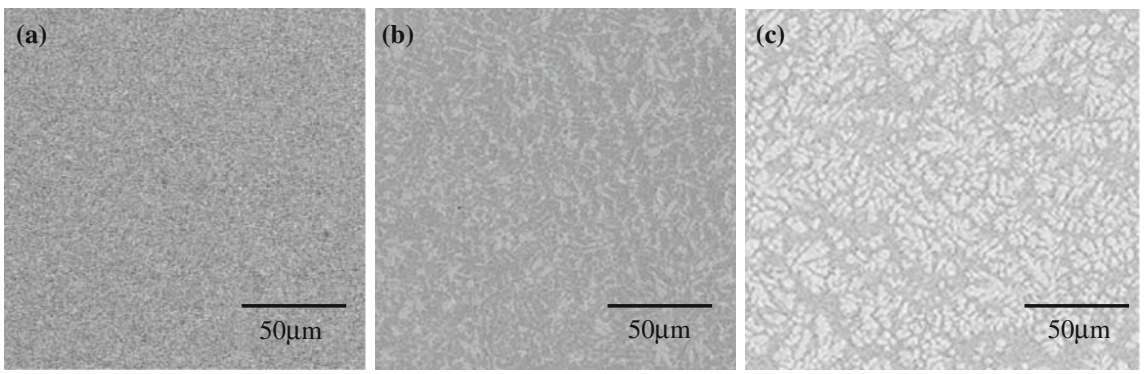

Fig. 2 SEM images of alloys with the different Nb concentrations **a** X = 0, **b** X = 5 and **c** X = 10

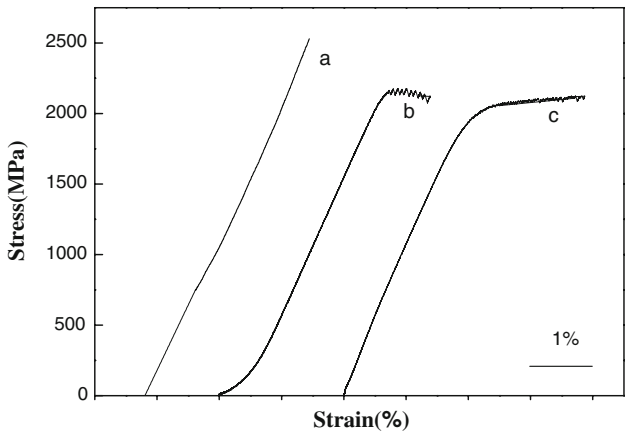

Fig. 3 Room temperature compression stress–strain plots for both the present composites containing (a) X = 0, (b) X = 5 and (c) X = 10

Table 1 The compressive mechanical properties of the current present composites

Alloy	σ_y (GPa)	σ_F^C (GPa)	ε_e (%)	ε_p (%)
0	2.5	2.5	2.3	0
5	2.15	2.1	2.2	1
10	2.0	2.1	2	2

testing conditions. It can be that these two alloys display an initial elastic deformation behavior with an elastic strain 2%, then begin to yield at about 2.15 and 2.0 GPa, respectively, followed by some strain hardening deformation. The compressive plastic strains of the alloys with 5% Nb and 10% Nb before fracture are 1 and 2%, respectively. The mechanical properties of all the samples are list in Table 1. By comparing the data in Table 1, one can see that the addition of Nb to the alloy led to the change of microstructure from fully amorphous to the composite with the dentritic crystalline phase, and consequently resulted in a decrease in yield and facture strength, but contributed to an increase in the plasticity, and with the increase of Nb content, the plasticity of the alloy increased with a slight loss of strength. These results are in agreement with the experimental reports in Ref. [16, 17], although the improvement in plasticity by adding Nb in this study is not too much high. This may be attributed to the casting processing effect in the present alloys, or to the different size and morphology of β-Zr phases between these alloys.

Figure 4 shows the SEM fractographies of all the samples, and the angle θ between the compressive fracture surface and the stress axis were marked in this figure. It can be seen that the fracture of all the samples occurs in a shear mode, but the fracture angle decreases with the increase of the Nb content. The fracture angles for the alloys with Nb content of 0, 5 and 10%, are 40°, 35° and 28°, respectively, as seen in Fig. 4a, b and c. It is well documented that plastic deformation in amorphous alloys at room temperature is accommodated through the development of multiple shear bands, and is highly localized in very thin shear bands, but, in most cases, the fracture of BMGs did not proceed along the maximum shear plane, The fracture angle is in the range of 50–65° under tensile load, while is 40–45° under compressive load [16–18]. The deviation of the fracture angle of BMGs from 45° has been explained by taking the effect of the normal stress into account [18–20], and as a result, the plastic deformation of BMGs follows the Mohr–Coulomb criterion rather than the von Mises criterion, which is given by

$$\tau_c = \tau_0 + \alpha\sigma_n \tag{1}$$

Here, τ_0 is a constant, and $\propto$ is a system specific coefficient that controls the strength of the normal stress effect [18, 21], which can be given implicitly by [17]

$$\alpha = \frac{\cos(2\theta)}{\sin(2\theta)} \tag{2}$$

For the alloys with Nb content of 0, 5 and 10%, the measured angles are 40°, 35° and 28°, respectively. Therefore, the constants α_0, α_5 and α_{10} for the three alloys can be calculated as follows:

$$\alpha_0 = \frac{\cos(2\theta)}{\sin(2\theta)} = 0.176 \tag{2a}$$

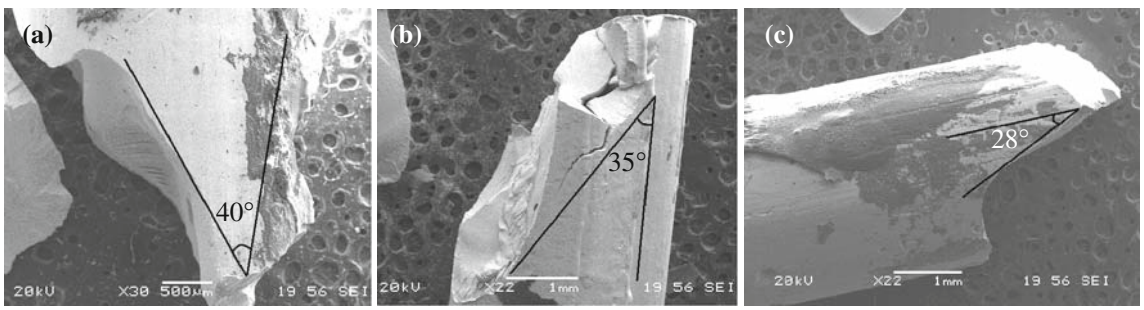

Fig. 4 SEM images of fracture angle for specimens with the different Nb concentrations **a** X = 0, **b** X = 5 and **c** X = 10

$$\alpha_5 = \frac{\cos(2\theta)}{\sin(2\theta)} = 0.364 \quad (2b)$$

$$\alpha_{10} = \frac{\cos(2\theta)}{\sin(2\theta)} = 0.673 \quad (2c)$$

Obviously, the constant for the single amorphous phase is much smaller than that for the composite, and with the increase of the volume fraction of the precipitated crystalline phase, the constant increases. It implies that the normal compressive stress should play a more remarkable role in the fracture process of the present composites than the fully amorphous alloy. This can be attributed to the interactions between the precipitated crystalline phase and the amorphous, and these interactions should contribute to the effect on the normal stress on the fracture process of the alloys.

Physically, the form of Eq. 1 was originally proposed for granular materials, where the σ_n term arises from the geometric rearrangement of sliding particles and the friction between them, thus $\propto$ is an effective coefficient of friction. It means that the precipitated crystalline phase in the composites effectively block the shear deformation and the fracture of the amorphous matrix. This study provided direct evidence that the constant $\propto$ can be regarded as an external reflection of the interactions among particles and the amorphous matrix. In turn, those interactions affect the deformation fracture mechanism of the metallic glass composite, and improve its mechanical properties, such as strength and ductility.

Moreover, the shear band morphologies on the surfaces of the alloys with the different Nb contents were examined on a SEM, as shown in Fig. 5. On the whole, the shear bands with low density near the fracture surface of the Nb-free alloy were arranged in an angle of 45° to the compressive load direction, whereas a small amount of shear bands nearly perpendicular to the compressive load direction caused by the casting defects were also observed, as shown in Fig. 5a. In contrast, the quantity of shear bands significantly increased in alloy with 5% Nb content, and these shear are parallel at nearly 45° to the compressive axis. In addition, some shear band branches can also be observed. With the increase of the Nb content, the density of the shear band increases, and these shear bands intersect and branch to form an intricate network. These shear band morphologies imply that the precipitated crystalline phase can effective block the shear band propagation, resulting in a delocalization of neighboring undeformed regions. The shear delocalization is expected to enhance the ductility of the composite.

Conclusions

In this study, the composites reinforced by in situ precipitated crystalline phase were successfully prepared by adding Nb in $Zr_{55}Cu_{15.5}Al_{7.5}Ni_{10}Be_{12}$ metallic glass. It was found that the addition of Nb in $Zr_{55}Cu_{15.5}Al_{7.5}Ni_{10}Be_{12}$ alloy led to the in situ precipitation of dendritic crystalline

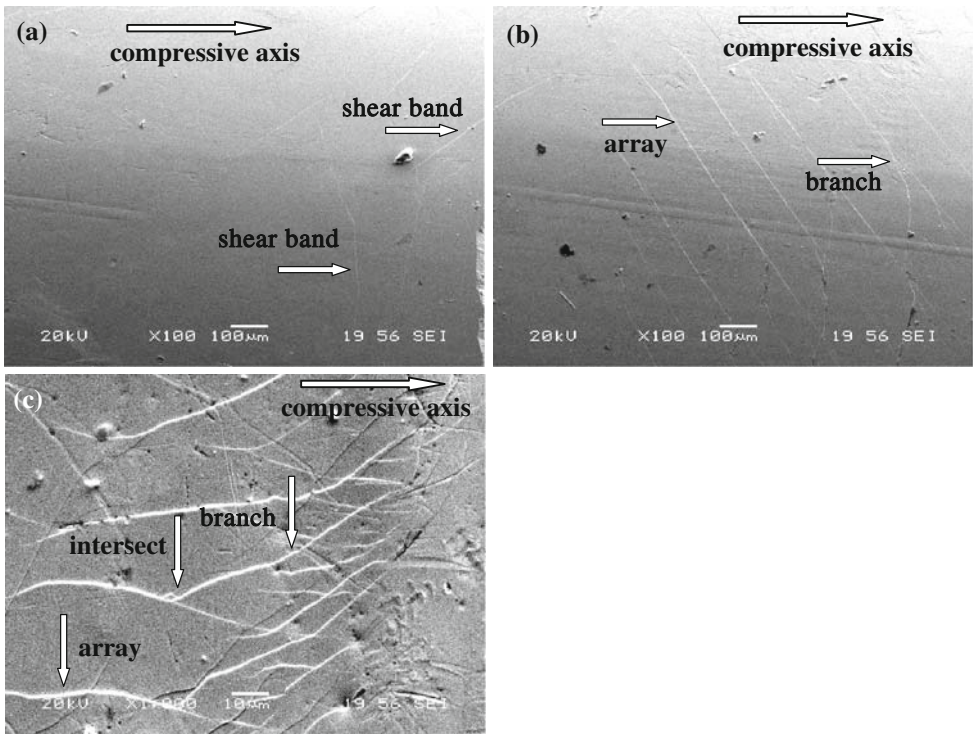

Fig. 5 SEM images of surface for specimens with the different Nb concentrations **a** X = 0, **b** X = 5 and **c** X = 10

β-Zr phase, and with the increase of Nb content, the size and the volume fraction of the dendritic precipitated phase increased. The composites exhibited a significant improvement of plasticity with a slight strength loss, compared to the fully amorphous $Zr_{55}Cu_{15.5}Al_{7.5}Ni_{10}Be_{12}$. The presence of the dentritic crystalline phase affect the deformation mechanism and fracture mode of the BMG by enhancing the affecting level of the normal stress on the shear surface, and the constant $\propto$ in the Mohr–Coulomb criterion can reflect the extent of the interactions among particles and the amorphous matrix. Thus, the interaction between the precipitated phase and the shear band are responsible for the plasticity enhance of the composites.

Acknowledgements The authors would like to acknowledge financial support from the Hunan Science Foundation grant (No. 05JJ30110), the National Natural Science Foundation of China (No. 10872177), State Key Lab of Advanced Metals Materials (No. EG512677781CN), and the Scientific Research Fund of Hunan Provincial Education Department (No. 08A068).

References

1. Schuh CA, Hufnagel TC, Ramamurty U (2007) Acta Mater 55:4067
2. Inoue A et al (2000) Acta Mater 48:279
3. Wang WH, Dong C, Shek CH (2004) Mater Sci Eng R 44:45
4. Fan C, Louzguine DV, Li CF, Inoue A (1999) Appl Phys Lett 75:341
5. Fu XL, Lia Y, Schuh CA (2007) Scripta Mater 56:617
6. Lee JC, Kim YC, Ahn JP et al (2005) Acta Mater 53:129
7. Sun YF, Guan SK, Wei BC et al (2005) Mater Sci Eng A 406:57
8. Bian Z, Pan MX, Zhang Y, Wang WH (2002) Appl Phys Lett 81:4739
9. Saida J, Deny A, Setyawan H et al (2005) Appl Phys Lett 87:151907
10. Inoue A, Kimura HM, Zhang T (2000) Mater Sci Eng A 294–296:727
11. Liu CT et al (1998) Metall Mater Trans A 29:1811
12. Megusar J, Argon AS, Grant NJ (1979) Mater Sci Eng 38:63
13. Mukai T et al (2002) Scripta Mater 46:43
14. Sun GY, Chen G, Chen GL (2007) Intermetallics 15:632
15. Hays CC, Kim CP, Johnson WL (2000) Phys Rev Lett 84:2901
16. Pan DG, Zhang HF, Wang AM, Hu ZQ (2006) Appl Phys Lett 89:261904
17. Hofmann DC, Suh JY, Wiest A, Duan G, Lind ML, Demetriou MD, Johnson WL (2008) Nature 451:1085
18. He G, Zhang ZF, Löser W, Eckert J, Schultz L (2003) Acta Mater 51:2383
19. Zhang ZF, He G, Eckert J, Schultz L (2003) Phys Rev Lett 91:045505
20. Zhang ZF, Eckert J, Schultz L (2003) Acta Mater 51:1167
21. Christopher AS, Alan CL (2003) Nat Mater 2:449